Research Article

Comparative study of statistical and soft computing-based predictive models for material removal rate and surface roughness during helium-assisted EDM of D3 die steel

Nishant K. Singh[1] · Yashvir Singh[2] · Sanjeev Kumar[3] · Abhishek Sharma[4]

Abstract
This research work proposes mathematical models, based on artificial neural network (ANN) with back-propagation algorithm, adaptive neuro-fuzzy inference system (ANFIS) and response surface methodology (RSM), for prediction of material removal rate (MRR) and surface roughness (SR) of helium-assisted electrical discharge machining of D3 die steel. The helium gas-assisted die-sinking EDM with perforated electrode was carried out by an EDM machine. For the present experimental work, discharge current, pulse on time, duty cycle, electrode rotation and discharge gas pressure were selected as process factors, while MRR and SR were chosen as process responses. Analysis of variance (ANOVA) was done to examine the adequacy of the developed model. The fit summary confirmed that the quadratic model is statistically appropriate and the lack of fit is insignificant. Root mean square error and absolute standard deviation, obtained through RSM, were also used for developing the model and for its predicting abilities through ANN and ANFIS. The experimental and predicted values of MRR and SR during the process, obtained by RSM, ANN and ANFIS, were found to be in accord with each other. However, the ANFIS technique proved to be more fitting to the responses as compared to the ANN and the RSM. The optimum value of the MRR at 28.54 mg/min and the SR at 4.21 μm was obtained with optimal process parameters by optimization of developed statistical models using genetic algorithm.

Keywords Helium · Assisted · RSM · ANN · ANFIS · CCRD · Model

1 Introduction

Electrical discharge machining (EDM) is a widely used non-conventional machining process, which utilizes heat from sparks to remove materials from stiff and hard work pieces which cannot be machined by conventional methods. The process is used for fabrication of molds, dies, automotive and aeronautical components [1]. However, moderate material removal rate (MRR), excessive tool wear rate (TWR) and substandard surface quality are major shortcomings of the EDM process that are yet to be resolved. While it is an important means for machining hard materials and ceramic composites, one also has to keep in mind that productivity with a high level of accuracy is always a matter of priority in any process and EDM lacks in that aspect [2]. Researchers have long been engaged to find ways for improving the MRR. Some of the widely used methods include high pressure gas flow through thin-walled pipe tool electrode, ultrasonic-assisted EDM, rotary EDM with ball burnishing, vibratory electrode and a rotary electrode, integration of work piece vibration and tool vibration with electrode rotation, electrodes with peripheral slots, ultrasonic-assisted cryogenically cooled electrode, etc.

✉ Nishant K. Singh, nishant.singh78@gmail.com | [1]Department of Mechanical Engineering, Hindustan College of Science and Technology, Mathura, UP, India. [2]Department of Mechanical Engineering, Sir Padampat Singhania University, Udaipur, Rajasthan, India. [3]Department of Electrical Engineering, Hindustan College of Science and Technology, Mathura, UP, India. [4]Department of Mechanical Engineering, G L Bajaj Institute of Technology and Management, Greater Noida, UP, India.

SN Applied Sciences (2019) 1:529 | https://doi.org/10.1007/s42452-019-0545-x

Received: 9 March 2019 / Accepted: 29 April 2019 / Published online: 6 May 2019

1.1 Literature review with aspects of improved machining performance of EDM

Mohan et al. [3] investigated the influence of tool rotation on the machinability of EDM operation. They conducted impact analysis of a conventional stationary electrode and a rotary electrode on output responses. Kuppan et al. [4] carried out investigations to analyze the influence of tool rotation during the EDM drilling of Inconel 718. Teimouri and Baseri [5] studied impelled action of tool rotations and different intensities of magnetic field on EDM machining. They compared the machining performance of the conventional EDM and the magnetic field-assisted rotary EDM with the same processing parameters. Abdulkareem et al. [6] carried out experimentation to study the effect of cryogenic cooled electrode on process responses during EDM of titanium alloy work piece. Srivastava and Pandey [7] investigated the effect of ultrasonic-assisted cryogenically cooled tool on machinability of the EDM process. They compared the effectiveness of the concerned electrode with a conventional electrode as well as with a cryogenically cooled electrode in terms of process responses. Aliakbari and Baseri [8] applied the Taguchi-based design of experiment (DOE) to obtain the optimum process factors for rotary-assisted multi-hole electrode EDM process. The authors also studied the effect of machining factors on responses, such as SR, MRR, EWR and overcut. Gu et al. [9] did a feasibility analysis of EDM on Ti6Al4 V by using bundled electrode. They also undertook a comparative analysis of process responses by using bundled tool and by using conventional solid tool while conducting EDM operation. Singh et al. [10] studied the effect of air-assisted multi-hole rotary tool electrodes during the EDM process. They found that its use improved the MRR and reduced the EWR as compared to solid rotary tool electrodes under the same machining conditions.

1.2 Literature review in correlation of soft computing model development

In the last few decades, various researchers have proposed different modeling tools to establish a correlation between machining parameters and prominent output responses like MRR and SR. Mandal et al. [11] used ANN to develop models to study the MRR and the absolute tool wear rate. Further, they applied a non-dominating sorting genetic algorithm to find the optimum value of process responses. Assarzadeh and Ghoreshi [12] applied ANN to develop models and to get optimal value of responses, viz. the MRR and the SR, during the EDM operation. Pradhan et al. [13] proposed two different ANN-based models for prediction of the SR during the EDM process. Their finding established that back-propagation neural network model gives more accurate results than radial basis function neural network model. Pataowari et al. [14] developed models to determine average layer thickness and material transfer rate during EDM operation by applying ANN. Panda [15] used neuro-grey modeling approach for optimization of process responses, such as depth of heat-affected zone, SR, MRR and micro-hardness of machined surface. Kumar et al. [16] applied ANN paired with Taguchi technique for modeling and optimization of the SR. Kumar and Choudhury [17] used ANN techniques to determine the SR and wheel wear during Electrical Discharge Diamond Grinding (EDDG) of high-speed steel (HSS) specimen. They observed that ANN-based model makes more precise assessment in comparison with regression-based model. Agarwal et al. [18] developed models to determine the MRR and the SR during EDGC by applying an ANN method. Kar et al. [19] optimized the SR parameters during electrodischarge coating process by applying fuzzy logic coupled with the Taguchi technique. Unune et al. [20] used an ANN and RSM-based technique to develop a model for determining MRR and SR through EDGC of Inconel 718. Prakash et al. [21] obtained optimum value of the input parameters in powder mixed EDM by using the Taguchi-based RSM coupled with a non-dominated sorting genetic algorithm.

1.3 Research gaps and novelty of this study

- Very few studies have been performed on the application of liquid cum gaseous dielectrics in hybrid EDM, which would ensure better MRR and surface finish in gas-assisted EDM.
- Development of the statistical model while considering dielectric properties, such as discharge gas pressure and tool rotation speed for additional investigation, has not been addressed in the literature.
- Very few investigations are there on the comparison of statistical and soft computing models. Most of the researches have been focused on comparison of the soft computing models in EDM.
- A small number of studies have been performed for evaluation and prediction of EDM responses like MRR and SR using ANN and ANFIS modeling techniques.
- Comparative study among RSM, ANN and ANFIS models has not been addressed in the literature.

In view of the aforementioned issues, in the present work, hybrid EDM technique, using liquid–gaseous dielectrics, has been proposed to utilize the advantage of oil EDM as well as dry EDM. Compressed helium gas has been used in die-sinking EDM to prevent the oxidation reaction, chances of fire and hazards during the machining operation. Central composite rotatable design (CCRD) has also been used to plan the experimentation. Based on the obtained results, ANN, ANFIS and RSM-based models have been developed to assess the influence of various machining factors on MRR and SR during helium-assisted electrical discharge machining (HAEDM) process. Statistical analysis of the experimental data has been done using analysis of variance (ANOVA). ANOVA enables to get insight into the machining process and distinguish between the factors which have significant effects on the process responses. The efficacy of the established models in predications of machinability has been compared at the end. This type of study would assist in evolving a suitable model for simulation of the EDM process.

2 Experimentation

2.1 Aspects of work piece and tool materials

Experiments were conducted on D3 die steel, which is broadly utilized for making molds and dies. A rectangular work piece with dimensions of 20 mm × 15 mm × 15 mm was used along with a perforated tube as a tool electrode to ensure smooth flow of high-velocity gas through it. The work piece had hardness of 51HRC. Table 1 shows the chemical composition of the selected work piece.

2.2 Details of tool design

A schematic of the perforated tube electrode is presented in Fig. 1a. In order to ensure effective transfer of heat from tool tip, a tool having diameter of 8.35 mm and length of 70 mm was chosen. A review of literature disclosed that among all the parameters, it is the discharge parameters, viz. discharge current, pulse on time, duty cycle, tool speed and discharge gas pressure, that significantly influence the EDM operation. Accordingly, five factors were chosen for the present study. The experimentations were carried out involving these five factors at various levels. The values of these factors were selected on the basis of preparatory experiments and capacity of the machines. When reverse polarity was used (i.e., tool is at positive terminal and workpiece is at negative terminal), high energy electrons strike the workpiece and the positively charged ions strike the tool resulting in better material removal from workpiece. Therefore, experimentation is conducted with reverse polarity.

Details of machining parameters with their range are given in Table 2. The gas-assisted die-sinking EDM was conducted with a perforated tool. For all the experiments, machining time was fixed at 15 min. The dielectric medium, selected for the present experiment, was kerosene. Figure 1b illustrates the schematic of the experiment setup, developed to carry out the HAEDM process.

The present study examined effects of various process factors on output through the CCRD method. A total of 32 experiments were conducted using the CCRD method

Table 1 Chemical composition of specimen

Element	C	Si	Cr	Mn	P	S	Fe
wt. (%)	1.80	0.50	9.85	0.40	0.05	0.05	Rest

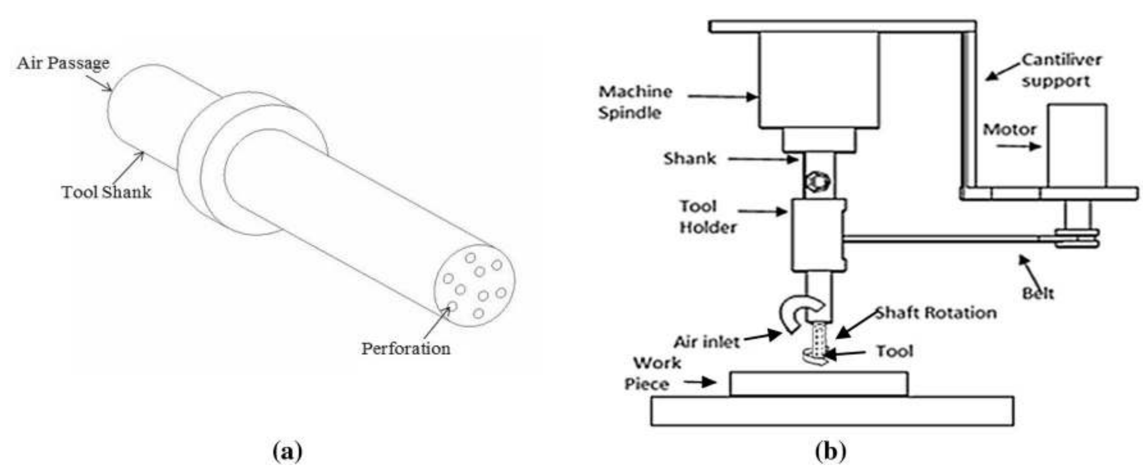

Fig. 1 Schematic diagram of **a** tool electrode **b** experiment setup mounted on EDM machine. [10]

Table 2 Process factors with ranges

Machining factors	Range
Discharge current (I_p) (A)	3,4,5,6,7
Pulse on time (T_{on}) (μs)	100,200,300,400,500
Duty cycle (DC)	0.52,0.58,0.64,0.70,0.76
Tool rotation speed (rpm)	200,400,600,800,1000
Gas pressure (GP) ($mmHg$)	4,8,12,16,20

with independent variables at 5 different levels. The machined specimens were cleaned with acetone. An electronic weighing balance (least count of 0.1 mg) was used for weight measurement. In order to ensure an accurate machining time calculations, electronic timer (accuracy of 0.1 s) was used. A portable SR tester, Mitutoyo (model: SJ 201P), was used to quantify the SR of the machined work piece.

3 Results and discussions

3.1 Analysis of variance (ANOVA)

Statistical analysis of the experimental findings was done by ANOVA. The ANOVA of a second-order model of the HAEDM process for the MRR and the SR is shown in Tables 3 and 4. The fit summary suggested that the quadratic model for the MRR and the SR is statistically appropriate and the lack of fit is not significant. For the model, the value of "Prob > F" is smaller than 0.05 (95% confidence). Therefore, it confirms that the parameters in the model have notable influence on the output responses. The value of R^2 shows that regression models have a proficient correlation between independent variables and the responses as well as offer a good explanation of this relationship. Equations 1 and 2 represent the statistical equations of the MRR and the SR, respectively.

Table 3 ANOVA results for MRR model (considering significant terms only)

Source	DF	Adj SS	Adj MS	F	P
Regression	20	514.691	25.735	51.53	0.000
Linear	5	472.897	94.579	189.38	0.000
Current	1	318.573	318.573	637.88	0.000
Ton	1	114.319	114.319	228.90	0.000
DC	1	8.120	8.120	16.26	0.002
Gas pressure	1	29.748	29.748	59.57	0.000
Square	5	23.483	4.697	9.40	0.001
Current*current	1	13.595	13.595	27.22	0.000
RPM*RPM	1	7.794	7.794	15.61	0.002
Interaction	10	18.311	1.831	3.67	0.020
DC*gas pressure	1	3.706	3.706	7.42	0.020
Ton* gas pressure	1	3.572	3.572	7.15	0.022
Residual error	11	5.494	0.499	–	–
Lack of fit	6	3.892	0.649	2.02	0.228
Pure error	5	1.602	0.320	–	–
Total	31	520.185	–	–	–

$S = 0.706698$, PRESS = 102.972, $R^2 = 98.92\%$, R^2 (pred) = 85.41%, R^2 (adj) = 97.02%

Table 4 ANOVA results for SR model (considering significant terms only)

Source	DF	Adj SS	Adj MS	F	P
Regression	20	5.34059	0.26703	39.27	0.000
Linear	5	3.77768	0.75554	111.12	0.000
Current	1	1.27882	1.27882	188.08	0.000
Ton	1	0.97607	0.97607	143.55	0.000
DC	1	0.79207	0.79207	116.49	0.000
RPM	1	0.60167	0.60167	88.49	0.000
Gas pressure	1	0.12907	0.12907	18.98	0.001
Interaction	10	1.49265	1.49265	21.95	0.000
Current*ton	1	0.10562	0.10562	15.53	0.002
DC*ton	1	0.04622	0.04622	6.80	0.021
Ton*RPM	1	0.04623	0.04623	6.80	0.021
DC*gas pressure	1	1.19902	1.19902	176.34	0.000
Residual error	11	0.07479	0.00680	–	–
Lack of fit	6	0.04546	0.00758	1.29	0.398
Pure error	5	0.02933	0.00587	–	–
Total	31	5.41539	–	–	–

$S = 0.0824588$, PRESS = 1.24377, $R^2 = 98.62\%$, R^2 (pred) = 77.71%, R^2 (adj) = 96.11%

$$\begin{aligned} \mathrm{MRR} = & -22.4 - \left(1.93 \times I_p\right) + \left(0.0120 \times T_{\mathrm{on}}\right) + (33.8 \times \mathrm{DC}) \\ & + (0.0141 \times \mathrm{RPM}) + (1.92 \times \mathrm{GP}) + \left(0.676 \times I_p^2\right) \\ & - \left(0.000013 \times \mathrm{RPM}^2\right) - \left(0.00394 \times I_p \times T_{\mathrm{on}}\right) \\ & - \left(0.00118 \times T_{\mathrm{on}} \times \mathrm{GP}\right) - (2.01 \times \mathrm{DC} \times \mathrm{GP}) \end{aligned} \tag{1}$$

$$\begin{aligned} \mathrm{SR} = & 3.38 - (0.013 \times I_p) - (0.0102 \times T_{\mathrm{on}}) + (0.34 \times \mathrm{DC}) \\ & + (0.00160 \times \mathrm{RPM}) + (0.0183 \times \mathrm{GP}) + (0.000812 \times I_p \times T_{\mathrm{on}}) \\ & + (0.0090 \times T_{\mathrm{on}} \times \mathrm{DC}) - (0.000003 \times T_{\mathrm{on}} \times \mathrm{RPM}) \end{aligned} \tag{2}$$

The normal distribution of residuals (refer Fig. 2) reveals that there is no distinct paradigm and uncommon structure. This suggests that the developed models are appropriate and can be used to examine significant influence of distinct factors on the process responses.

Contribution percentage of each parameter of the model to the MRR and the SR is depicted in Fig. 3. Figure 3a reveals that discharge current, pulse on time and

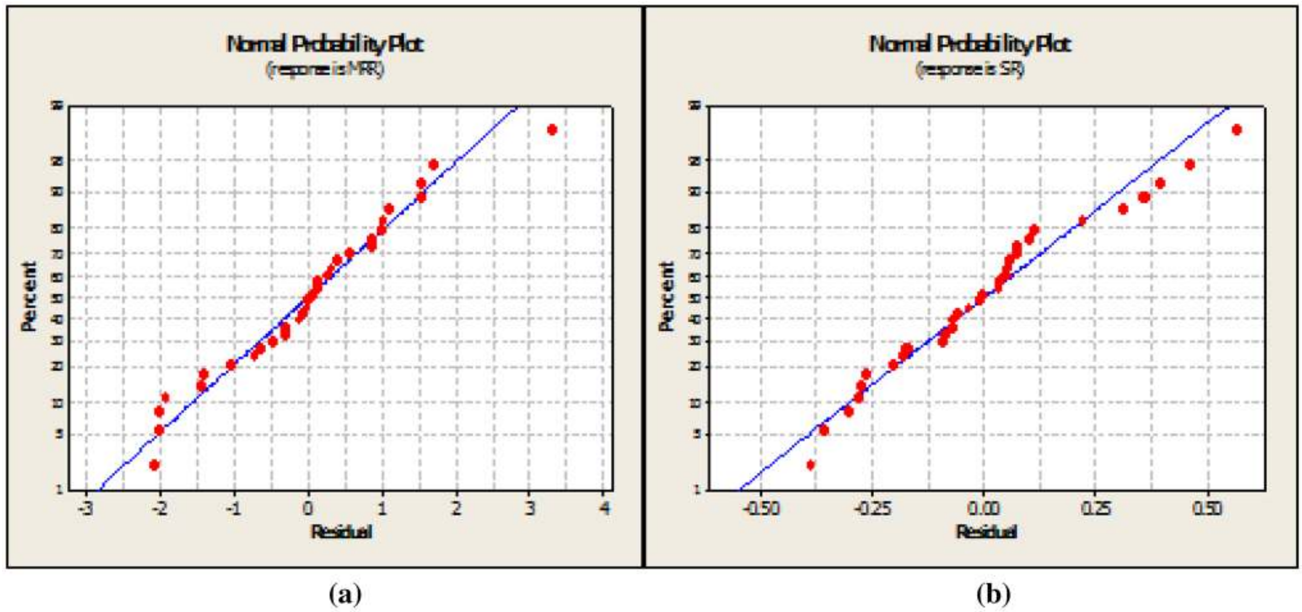

Fig. 2 Normal probability plot of **a** residual for MRR **b** residuals for SR

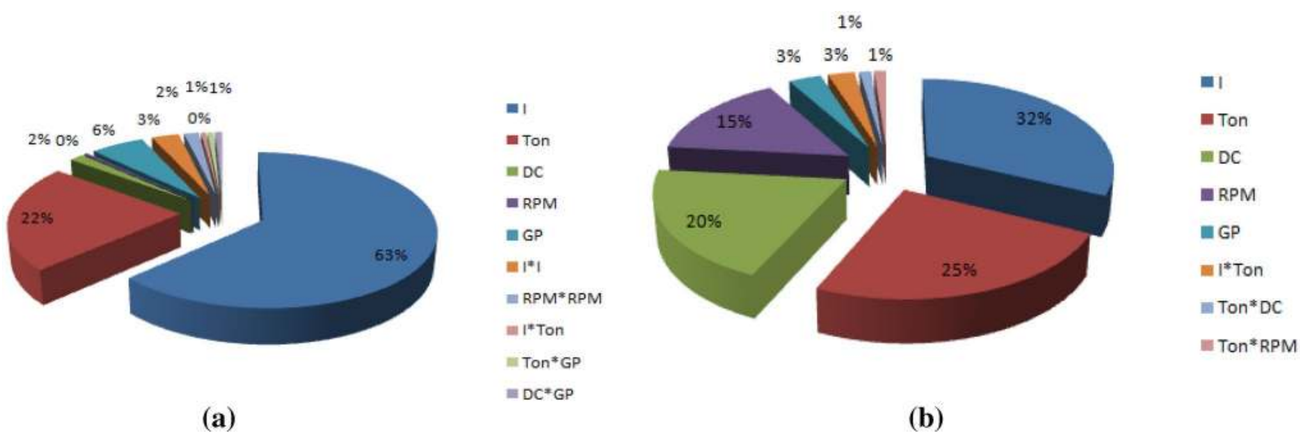

Fig. 3 Contribution (%) of each parameter **a** on MRR **b** on SR, for HAEDM

gas pressure are crucial parameters affecting the MRR. Of them, the discharge current is found to be the most notable parameter affecting the MRR with a contribution of 63%. Figure 3b reveals that discharge current, pulse on time, duty cycle and tool speed are critical factors influencing the SR. Out of them, discharge current is found to be the most notable factor influencing the SR with a contribution of 32%, which is followed by pulse on time and duty cycle with a contribution of 25% and 20%, respectively.

3.2 Effects of process parameters

Figure 4 shows the main effect plots for the MRR. It can be observed that the MRR increases with a rise in discharge current and duty cycle. Again, from the plot, it can be seen that the MRR gets reduced with an increase in pulse on time and tool speed. On the other hand, the MRR goes up with discharge gas pressure. It is probably the flushing efficiency of the process that improves with an enhancement in discharge gas pressure, which, in turn, contributes to a better MRR. However, high tool rotation results in an increased turbulence, which stirs up the plasma channel [25]. As a result, discharge energy decreases and leads to a lower MRR after tool speed reaches a certain value. Figure 5 presents the main effects plots for the SR. It can be seen that the SR increases with a rise in discharge current and duty cycle and reduces with a rise in pulse on time. The SR also shows an increase with discharge gas pressure

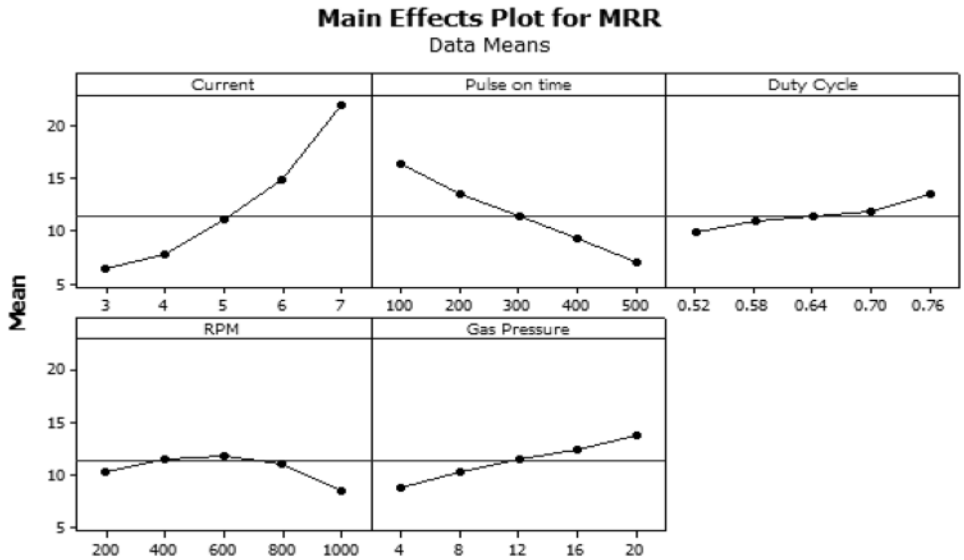

Fig. 4 Main effects plots for MRR

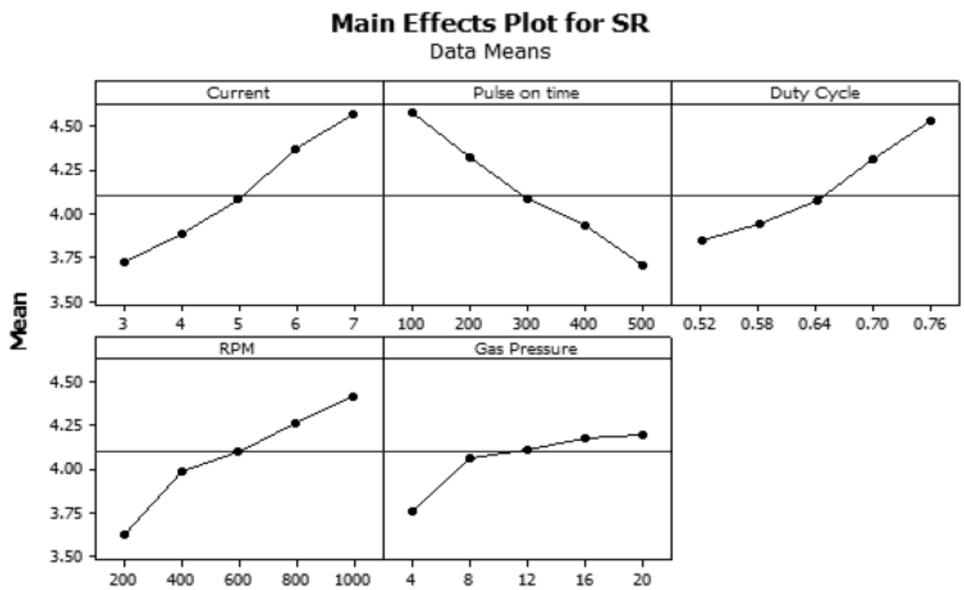

Fig. 5 Main effects plots for SR

and tool speed. When the tool rpm and discharge gas pressure are increased, the flushing action improves, resulting in low deposition of the recast layer. Low deposition of carbon leads to larger size craters, thereby enhancing the SR. Yan et al. [23] and Chattopadhyay et al. [24] in their investigations have also found the same effect of tool rotation during the EDM.

3.3 Prediction of MRR and SR in HAEDM

ANN is the most widely used soft computing technique to unravel complex nonlinear problems. This technique offers a flexibility of learning the mapping between the input factors and the process responses to sort out complicated problems [16]. The neural network consists of immensely interconnected neural computing elements. The neural elements have a competency to learn and extract information, and they are ready for use [20]. They can rehearse like human by gathering information during continuous learning pursuits. Because of these computational capabilities of ANN, it was chosen in the modeling of the HAEDM process. In the present work, the MATLAB software was used to design the best ANN architecture. The input layer corresponded to discharge

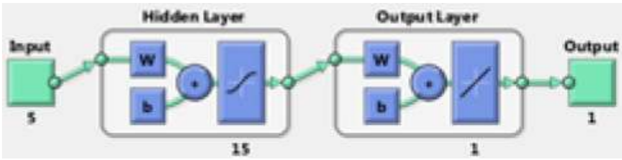

Fig. 6 ANN structure 5-15-1

current, pulse on time, duty cycle, tool speed and discharge gas pressure. The output layer corresponded to the MRR or the SR. In this model, the input layer is associated with a hidden layer neuron and the hidden layer is associated with output layers. After extensive trials and on the basis of functioning of the network, ANN models for the MRR and the SR were developed. In these models, one hidden layer consists of 15 neurons, 5 input and 1 output neurons as shown in Fig. 6. For swift and supervised learning, Levenberg–Marquardt back-propagation neural network algorithm was used during training of the network [14–16]. The network performance is measured using mean square error (MSE) and average error percentage. MSE can be calculated as:

$$\mathrm{MSE} = \frac{1}{X \times Y} \sum_{i=1}^{X} \sum_{j=1}^{Y} \left(p_j - q_j\right) \tag{3}$$

where X is the number of output nodes, Y is the total number of training data, p_j is output of the jth neuron and q_j is the predicted value of jth neuron [20].

In the present ANN model for the MRR and the SR during simulating, the values of correlation coefficients (R) are 0.9989 and 0.9986 as shown in Fig. 7. From the statistical point of view, a network can more precisely correlate the process input to the output response if the value of the correlation coefficients is closer to 1. Therefore, for a wide range of machining conditions, a selected BP neural network effectively maps the process factors for the process output responses [11]. Figure 8 shows the comparison of actual and predicted value of the MRR and the SR by FFBP-ANN. From the figure, one can observe an accord between the measured and the predicted values as attained by the FFBP-ANN models.

3.4 Prediction of MRR and SR in HAEDM by ANFIS

ANFIS is a hybrid model which integrates ANN's adaptive potential and fuzzy logic's qualitative techniques. ANFIS exploits the competency of the ANN and fuzzy logic and simultaneously prevails over their respective limitations [22]. In the present investigation, the ANFIS technique was applied to establish the correlation between input factors and output response, such as the MRR and the SR during

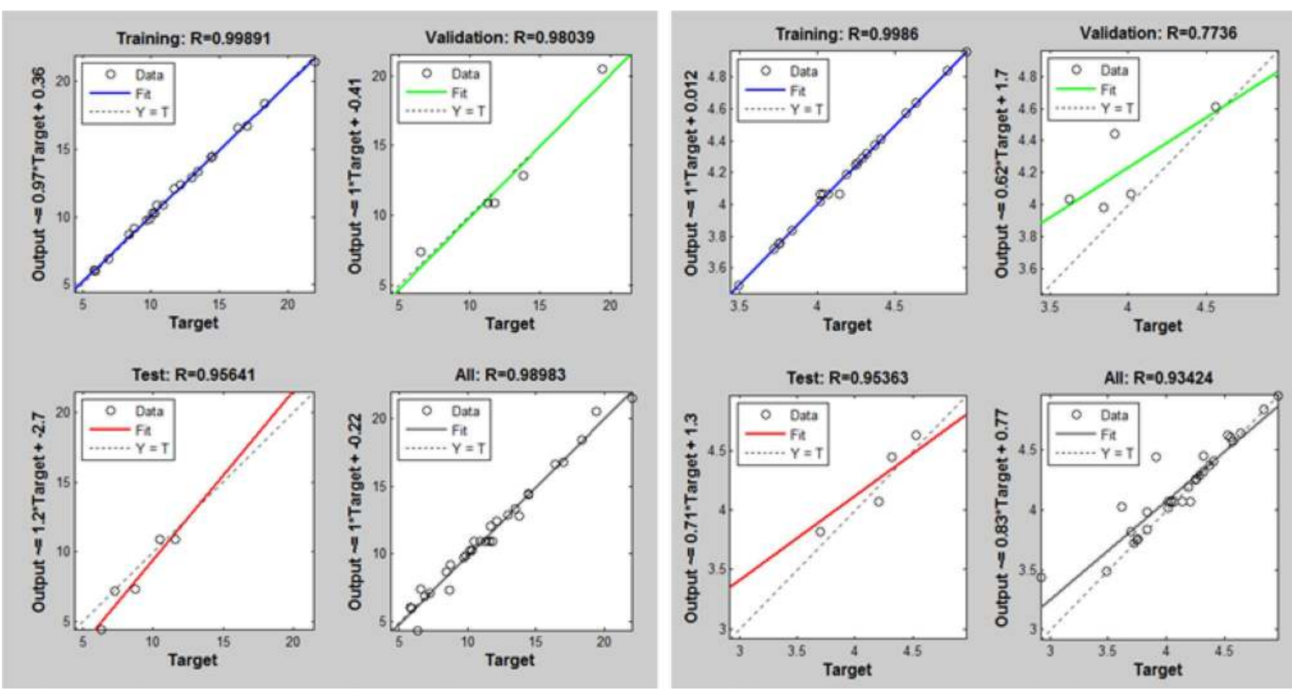

Fig. 7 Linear regression analysis between the experimental values and predicted values by FFBP-ANN for training, validation, testing and overall **a** of MRR **b** of SR

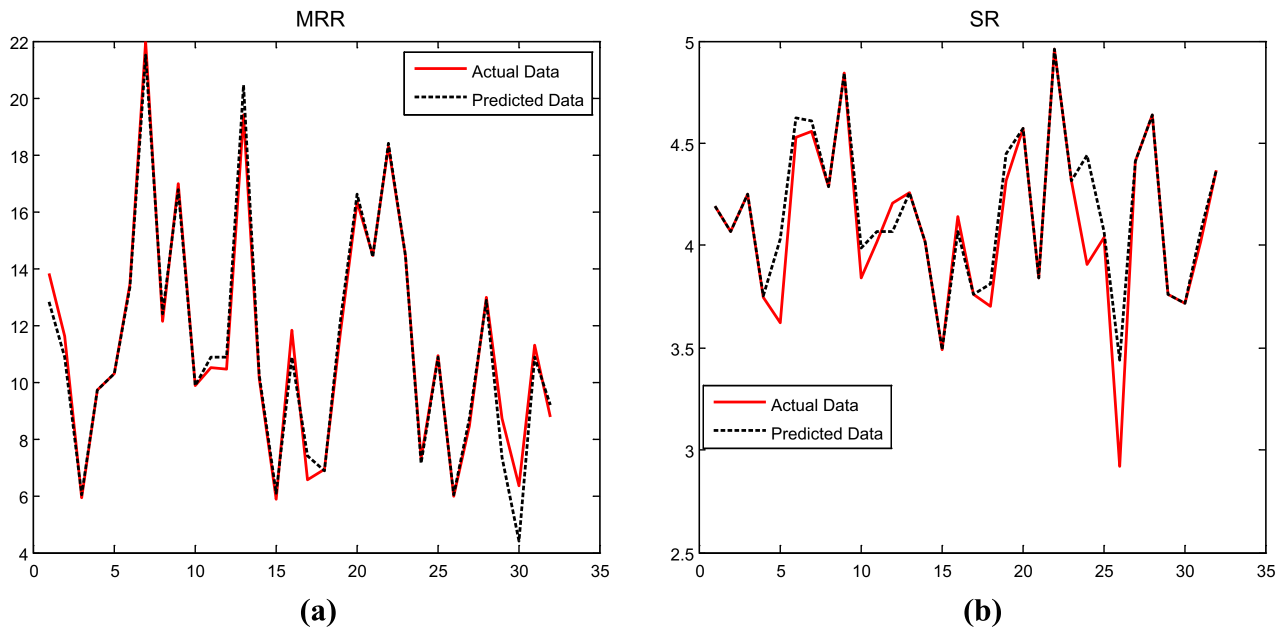

Fig. 8 Comparison of actual and predicted value by FFBP-ANN for **a** MRR **b** SR

Table 5 ANFIS architecture and training parameters

Number of nodes	524
Number of linear parameters	1458
Total number of parameters	1503
Number of training data pairs	24
Number of checking data pairs	8
Number of fuzzy rules	243
Membership function	Triangular

the HAEDM process. Modeling of process responses of the HAEDM process by ANFIS technique consists of two important stages: training and testing. For the ANFIS modeling, it is mandatory that all the process input factors should be quantitative. Here, as per the available design matrix 32 experiment data, a total of 24 data were arbitrarily selected for the training of ANFIS network. The remaining 8 data, which were not considered for training, were used for testing of the ANFIS model. The accuracy of the ANFIS model depends upon a few important factors, which are listed in Table 5.

Figure 9 shows that there is a good accord between the measured values of the MRR and the SR as well as the predicted values through the ANFIS model. From this figure, the developed models can be seen to have precisely predicted the value of the MRR and the SR. The precision of the prediction model was evaluated by using the root mean square error (RMSE) [20]. The following equation can be used to obtain the RMSE.

$$\mathrm{RMSE} = \sqrt{\frac{1}{T}\sum_{i=1}^{T}\left(X_i - Y_i\right)^2} \tag{4}$$

where T is the total training data, Xi is the value of the measured data and Yi is the value, predicted by the ANFIS model.

The prediction potential of any model can be determined only with an entirely new set of data. Hence, all the developed models were tested using a set of data, not previously used during the experimentation process. The set of data used for confirmation of experiments are listed in Table 6. The experimental and predicted results by RSM, ANN and ANFIS models were seen to have fewer fallacies. Thus, it can be confirmed that the developed models are appropriate and authentic in prediction of the MRR and the SR.

3.5 Comparison of predicted MRR and SR by ANN, ANFIS, and RSM

A comparison of predicted values of responses by RSM, ANN, and ANFIS models and measured values corresponding to each trial of the HAEDM process for the MRR and the SR is shown in Table 7. The precision of prediction

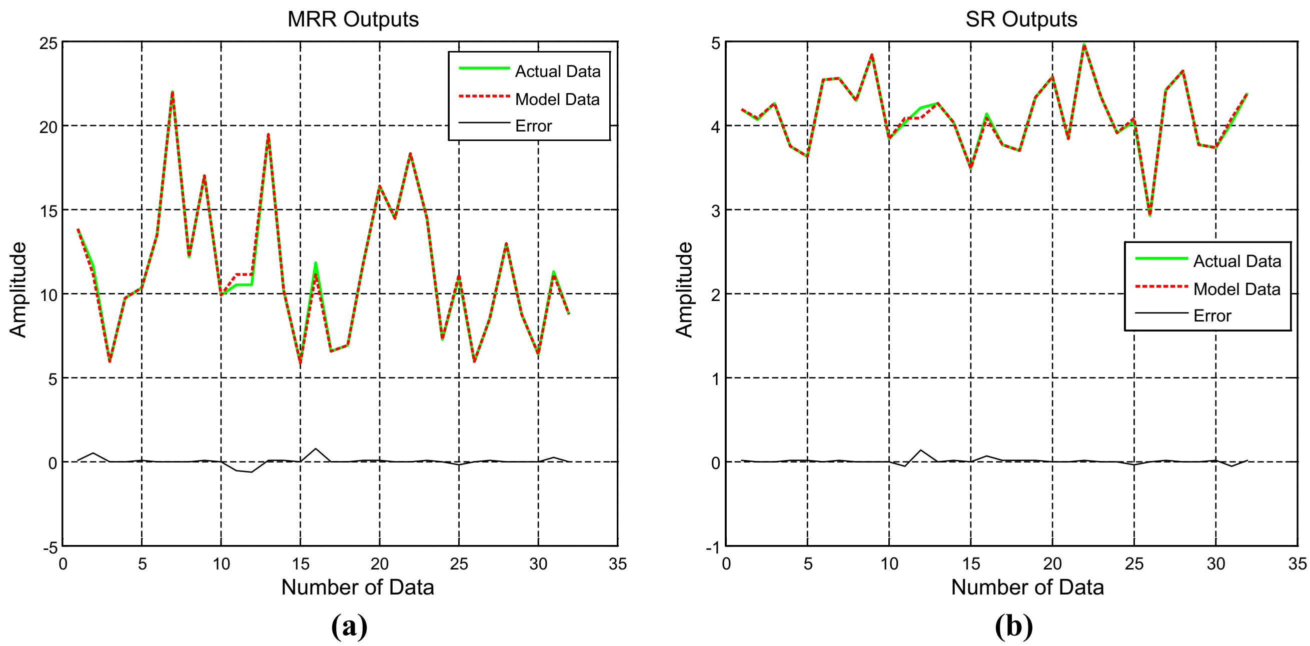

Fig. 9 Comparison of actual and predicted value by ANFIS for **a** MRR **b** SR

Table 6 Confirmation experiments

Exp. no.	Machining parameters					MRR (mg/min)				SR (μm)			
	I	Ton	DC	RPM	GP	Exp.	RSM	ANN	ANFIS	Exp.	RSM	ANN	ANFIS
1	7	300	0.58	600	20	24.02	23.93	24	24.02	4.52	4.48	4.48	4.52
2	4	100	0.64	400	12	11.75	11.70	11.74	11.75	4.26	4.17	4.21	4.26
3	5	200	0.76	200	8	12.62	12.55	12.60	12.62	4.10	4.06	4.2	4.10
4	6	300	0.70	600	16	15.77	16.85	16.74	16.76	4.68	4.54	4.61	4.69
5	5	300	0.64	400	12	11.22	11.09	11.20	11.21	4.12	3.92	4.09	4.10
RMS (error)	–	0.088	0.020	0.004	–	0.109	0.061	0.006					

model was assessed by using the standard deviation, mean square error (MSE), RMSE and is listed in Table 8. From these values, it can be concluded that the ANFIS model enables more authentic and precise prediction in comparison with RSM and ANN models. A comparison of experimental and predicted values of MRR and SR by ANN, ANFIS and RSM models is presented in Figs. 10 and 11, respectively.

3.6 Optimization of HAEDM process

So as to get the optimal machining parameters in HAEDM process, the multi- objective optimization was performed utilizing genetic algorithm strategy. The statistical response model of MRR and SR shown in Eqs. (1) and (2) for HAEDM process is utilized in the optimization. In the present work, the goal is to maximize MRR and minimize SR within the parameters range as mentioned in Table 2.

Minimize $f = f_1 + f_2^{-1}$,

where $f_1 = \mathrm{SR}$ and $f_2 = \mathrm{MRR}$

The Pareto-optimal front of non-dominated arrangement is appeared in Fig. 12. Figure 12 demonstrates a continuous Pareto-optimal front of non-dominated results, which shows that reasonable mixes of input parameters found in all the whole inquiry space. The

Table 7 Measured and predicted values of responses corresponding to each trial of HAEDM process

Exp. no.	I	Ton	DC	RPM	GP	MRR (mg/min)				SR (μm)			
						Exp.	RSM	ANN	ANFIS	Exp.	RSM	ANN	ANFIS
1	5	300	0.64	600	20	13.80	13.54	12.83	13.8	4.19	4.2	4.19	4.19
2	5	300	0.64	600	12	11.60	11.31	10.89	11.09	4.07	4.06	4.07	4.08
3	4	400	0.70	800	8	5.90	6.14	6.00	5.90	4.25	3.77	4.25	4.25
4	6	400	0.58	800	8	9.70	10.52	9.73	9.70	3.75	3.92	3.75	3.75
5	5	300	0.64	200	12	10.30	9.83	10.29	10.3	3.62	3.78	4.03	3.62
6	5	300	0.76	600	12	13.45	12.47	13.32	13.45	4.53	4.42	4.63	4.53
7	7	300	0.64	600	12	21.95	21.31	21.5	21.95	4.56	4.52	4.61	4.56
8	6	400	0.70	800	16	12.12	12.98	12.42	12.12	4.29	4.54	4.29	4.29
9	6	200	0.70	800	8	17.00	16.86	16.74	17.00	4.84	4.68	4.84	4.84
10	5	300	0.52	600	12	9.88	10.15	9.86	9.88	3.84	3.69	3.98	3.84
11	5	300	0.64	600	12	10.50	11.31	10.89	11.09	4.02	4.06	4.07	4.08
12	5	300	0.64	600	12	10.45	11.31	10.89	11.09	4.21	4.06	4.07	4.08
13	6	200	0.70	400	16	19.40	19.68	20.47	19.4	4.26	4.43	4.26	4.26
14	4	200	0.58	400	16	10.15	11.40	10.25	10.15	4.02	3.87	4.02	4.02
15	4	400	0.70	400	16	5.85	7.07	6.10	5.85	3.49	3.76	3.49	3.49
16	5	300	0.64	600	12	11.80	11.31	10.89	11.09	4.14	4.06	4.07	4.08
17	4	400	0.58	800	16	6.57	6.27	7.40	6.57	3.76	3.45	3.76	3.76
18	5	500	0.64	600	12	6.92	6.94	6.88	6.92	3.70	3.62	3.81	3.70
19	4	200	0.70	800	16	11.68	11.00	12.06	11.68	4.32	4.53	4.45	4.32
20	5	100	0.64	600	12	16.35	15.68	16.62	16.35	4.57	4.49	4.57	4.57
21	6	200	0.58	400	8	14.44	15.34	14.38	14.44	3.84	4.02	3.84	3.84
22	6	200	0.58	800	16	18.31	18.88	18.39	18.31	4.96	4.57	4.96	4.96
23	6	400	0.58	400	16	14.46	13.38	14.45	14.46	4.32	3.91	4.32	4.32
24	4	200	0.58	800	8	7.28	6.65	7.15	7.28	3.91	4.13	4.44	3.91
25	5	300	0.64	600	12	10.90	11.31	10.89	11.09	4.04	4.06	4.07	4.08
26	4	400	0.58	400	8	5.95	4.61	6.00	5.95	2.92	3.14	3.44	2.92
27	5	300	0.64	1000	12	8.43	8.63	8.69	8.43	4.41	4.34	4.41	4.41
28	6	400	0.70	400	8	12.96	13.25	12.87	12.96	4.64	4.24	4.64	4.64
29	5	300	0.64	600	4	8.71	9.07	7.34	8.71	3.76	3.91	3.76	3.76
30	3	300	0.64	600	12	6.35	6.72	4.39	6.35	3.72	3.60	3.72	3.72
31	5	300	0.64	600	12	11.30	11.31	10.89	11.09	4.02	4.06	4.07	4.08
32	4	200	0.70	400	8	8.77	9.38	9.17	8.77	4.37	3.98	4.37	4.37

Table 8 Precision of prediction models

Parameters	Model	MAE	MSE	RMSE	Standard deviation
MRR	RSM	0.5725	0.4530	0.6731	0.6796
	ANN	0.3906	0.3526	0.5938	0.5977
	ANFIS	0.0891	0.0501	0.2238	0.2273
SR	RSM	0.1778	0.0476	0.2181	0.2166
	ANN	0.0730	0.0255	0.1596	0.1504
	ANFIS	0.0113	$9.1875^{*}e^{-4}$	0.0303	0.0308

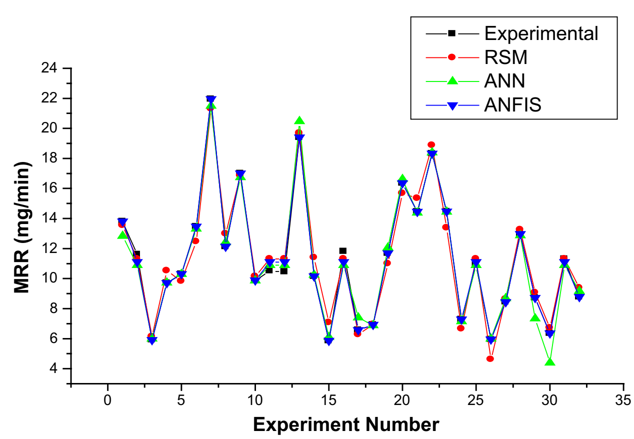

Fig. 10 Comparison of measured and predicted results of MRR for various models

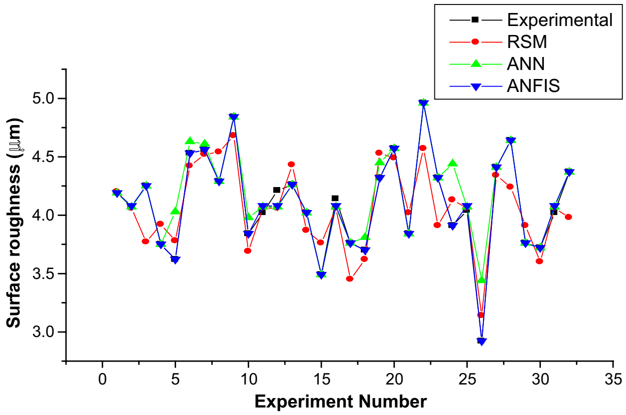

Fig. 11 Comparison of measured and predicted results of SR for various models

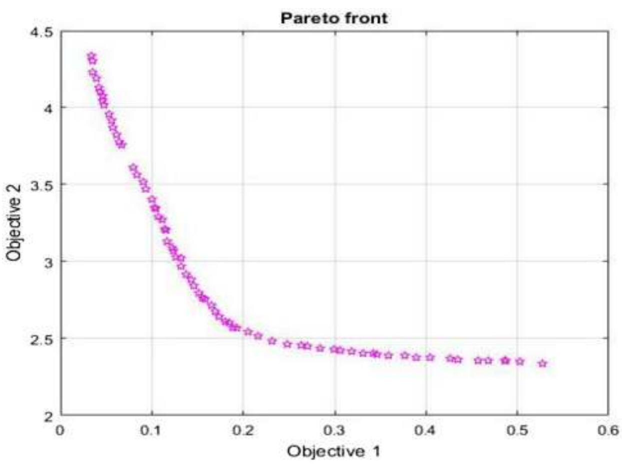

Fig. 12 Pareto-optimal front

optimal machining in HAEDM (discharge current 6A, pulse on time 158 µs, duty cycle 0.54, tool speed 291 rpm and gas pressure 19 mm of Hg) has been found to produce MRR and SR equivalent to 28.54 mg/min and 4.21 µm, respectively (Table 9).

4 Conclusions

In the present work, an experimental setup was successfully created to carry out the HAEDM process to measure process responses like the MRR and the SR. This work provides insights about the better prediction precision in EDM process; an improved perspective is suggested to model MRR and SR with ANN and ANFIS techniques, using RSM design of experimental techniques. The CCRD-based experiment design was used to analyze the effect of different parameters on the machining process. The ANN, ANFIS and RSM-based methods were used to develop models for predicting the MRR and the SR during the HAEDM process on D3 die steel.

The following are the key findings from the study that can be summed up:

- An RSM-based mathematical model was developed to predict the MRR and the SR during the HAEDM process. The predicted value of responses by the model was found to be in accord with the measured value of each experiment.
- The ANOVA was applied to examine adequacy of the developed model. The fit summary confirmed that the model is statistically appropriate and the lack of fit is insignificant.
- Two soft computing-based models, i.e., FFBP-ANN and ANFIS, were also developed for prediction of the HAEDM process performance. Due to lower values of the average error, MSE and RMSE soft computing-based models were found to predict more accurately as compared to the mathematical RSM model.
- For validation of the RSM, ANN and ANFIS models, confirmatory experiments were carried out. All the three models predicted the MRR and SR accurately.
- A comparison was done among the developed models to identify the most precise one among the three. The ANN-based model outperformed the mathematical RSM model in general. However, ANFIS model was found to predict responses most precisely as compared to ANN and RSM models.
- The optimal machining in HAEDM (discharge current 6A, pulse on time 158 µs, duty cycle 0.54, tool speed 291 rpm and gas pressure 19 mm of Hg) has been found to produce MRR and SR equivalent to 28.54 mg/min and 4.21 µm, respectively.

Table 9 Optimum set of parameters for MRR and SR

I	Ton	DC	RPM	GP	Predicted		Experimented		Error (%)	
					MRR	SR	MRR	SR	MRR	SR
6	158	0.54	291	19	28.54	4.21	29.63	4.14	3.81	1.66

Compliance with ethical standards

Conflict of interest The authors declare that they have no conflict of interest.

References

1. Ho KH, Newman ST (2003) State of the art electrical discharge machining (EDM). Int J Mach Tools Manuf 43:1287–1300
2. Singh NK, Pandey PM, Singh KK, Sharma MK (2016) Steps towards green manufacturing through EDM process: a review. Cogent Eng 3:1272662
3. Mohan B, Rajadurai A, Satyanarayana KG (2002) Effect of sic and rotation of electrode on electric discharge machining of Al–Si composite. J Mater Process Technol 124:297–304
4. Kuppan P, Rajadurai A, Narayanan S (2008) Influence of EDM process parameters in deep hole drilling of Inconel 718. Int J Adv Manuf Technol 38:74–84
5. Teimouri R, Baseri H (2012) Effects of magnetic field and rotary tool on EDM performance. J Manuf Process. https://doi.org/10.1016/j.jmapro.2012.04.002
6. Abdual Kareem S, Khan AA, Konneh M (2009) Reducing electrode wear ratio using cryogenic cooling during electrical discharge marching. Int J Adv Manuf Technol 45:1146–1151
7. Srivastava V, Pandey PM (2012) Effect of process parameters on the performances of EDM process with ultrasonic assisted cryogenically cooled electrode. J Manuf Process 14:393–402
8. Aliakabari E, Baseri H (2012) Optimization of machining parameters in rotary EDM process by using the Taguchi method. Int J Adv Manuf Technol 62(9–12):1041–1053
9. Gu L, Li L, Zhao W (2012) Electrical discharge machining of Ti6Al4V with a bundled electrode. Int J Mach Tools Manuf 53:100–106
10. Singh NK, Pandey PM, Singh KK (2016) EDM with air assisted multi-hole rotating tool. Mater Manuf Process 31(14):1872–1878
11. Mandal D, Pal Surjya K, Saha P (2007) Modeling of electrical discharge machining process using back propagation neural network and multi-objective optimization using non-dominating sorting genetic algorithm-II. J Mater Process Technol 186:154–162
12. Assarzadeh S, Ghoreishi M (2008) Neural-network-based modeling and optimization of the electro-discharge machining process. Int J Adv Manuf Technol 39:488–500
13. Pradhan MK, Das R, Biswas CK (2009) Comparisons of neural network models on surface roughness in electrical discharge machining. Proc. Inst Mech Eng Part B J Eng Manuf 223:801–808
14. Patowari PK, Saha P, Mishra PK (2010) Artificial neural network model in surface modification by EDM using tungsten–copper powder metallurgy sintered electrodes. Int J Adv Manuf Technol 51:627–638
15. Panda DK (2010) Modelling and optimization of multiple process attributes of electro discharge machining process by using a new hybrid approach of neuro-grey modeling. Mater Manuf Process 25:450–461
16. Kumar S, Batish S, Singh R, Singh TP (2014) A hybrid Taguchi-artificial neural network approach to predict surface roughness during electric discharge machining of titanium alloys. J Mech Sci Technol 28(7):2831–2844
17. Kumar S, Choudhury SK (2007) Prediction of wear and surface roughness in electro-discharge diamond grinding. J Mater Process Technol 191:206–209
18. Agrawal SS, Yadava V (2013) Modeling and prediction of material removal rate and surface roughness in surface-electrical discharge diamond grinding process of metal matrix composites. Mater Manuf Process 28:381–389
19. Kar S, Chakraborty S, Dey V, Ghosh SK (2017) Optimization of surface roughness parameters of Al-6351 alloy in EDC process: a Taguchi coupled fuzzy logic approach. J Inst Eng India Ser. https://doi.org/10.1007/s40032-016-0297-y
20. Unune DR, Mali HS (2016) Artificial neural network–based and response surface methodology–based predictive models for material removal rate and surface roughness during electro-discharge diamond grinding of Inconel 718. Proc Inst Mech Eng Part B J Eng Manuf. https://doi.org/10.1177/0954405415619347
21. Prakash C, Kansal HK, Pabla BS, Puri S (2016) Multi-objective optimization of powder mixed electric discharge machining parameters for fabrication of biocompatible layer on β-Ti alloy using NSGA-II coupled with Taguchi based response surface methodology. J Mech Sci Technol 30(9):4195–4204
22. Pradhan MK, Biswas CK (2010) Neuro-fuzzy and neural network-based prediction of various responses in electrical discharge machining of AISI D2 steel. Int J Adv Manuf Technol 50:591–610
23. Yan BH, Wang CC, Liu WD, Huang FY (2000) Machining characteristics of Al_2O_3/6061Al composite using rotary EDM with a disk like electrode. Int J Adv Manuf Technol 16:322–333
24. Chattopadhyaya KD, Verma S, Satsangi PC (2009) Development of empirical model for different process parameters during rotary electrical discharge machining of copper–steel (EN-8) system. J Mater Process Technol 209:1454–1465
25. Zhao W, Li L, Gu L (2012) Influence of flushing on performance of EDM with bunched electrode. Int J Mach Tools Manuf 58:187–194